

# Lanthanide–Transition-Metal Carbonyl Complexes. 1. Syntheses and Structures of Ytterbium(II) Solvent-Separated Ion Pairs and Isocarbonyl Polymeric Arrays of Tetracarbonylcobaltate

Christine E. Plečnik, Shengming Liu, Jianping Liu, Xuenian Chen, Edward A. Meyers, and Sheldon G. Shore\*

Department of Chemistry, The Ohio State University, Columbus, Ohio 43210

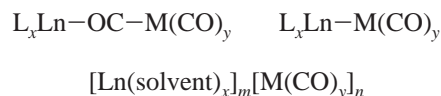
Received April 2, 2002

Transmetalation reactions of metallic ytterbium with  $\text{Hg}[\text{Co}(\text{CO})_4]_2$  in the coordinating solvents pyridine and THF yield the solvent-separated ion pairs  $[\text{Yb}(\text{L})_6][\text{Co}(\text{CO})_4]_2$  (**1a**, L = Pyr; **2a**, L = THF). The IR spectrum of **1a** in pyridine indicates that the tetracarbonylcobaltate anion is not directly bonded to the divalent Yb cation owing to the strong coordinating ability of pyridine. On the other hand, IR spectra of **2a** in THF are concentration dependent. In dilute solutions there is an equilibrium between the solvent-separated ion pair and a weak contact ion pair. Higher concentrations of **2a** facilitate the formation of a tight ion pair that has a low-frequency isocarbonyl absorption. Remarkably, complexes **1a** and **2a** are easily transformed in toluene into the two-dimensional sheetlike arrays  $[(\text{Pyr})_4\text{Yb}\{(\mu\text{-CO})_2\text{Co}(\text{CO})_2\}_2]_\infty$  (**1b**) and  $[(\text{THF})_2\text{Yb}\{(\mu\text{-CO})_3\text{Co}(\text{CO})\}_2\cdot\text{Tol}]_\infty$  (**2b**). The two-dimensional frameworks are supported by isocarbonyl linkages. Infrared spectra of toluene solutions substantiate the existence of the isocarbonyl bridges with low-frequency absorptions at  $1780\text{ cm}^{-1}$ . Compounds **1b** and **2b** belong to a rare class of lanthanide–transition-metal carbonyl extended arrays, only three others of which have been structurally established. Dissolving **1b** in pyridine regenerates **1a**, but the complete conversion of **2b** into **2a** cannot be achieved. Crystal data: **1a**·Pyr is monoclinic,  $P2_1/c$ ,  $a = 11.171(1)\text{ \AA}$ ,  $b = 11.925(1)\text{ \AA}$ ,  $c = 33.978(1)\text{ \AA}$ ,  $\beta = 95.10(1)^\circ$ ,  $Z = 4$ ; **2a** is monoclinic,  $C2/c$ ,  $a = 17.724(1)\text{ \AA}$ ,  $b = 12.468(1)\text{ \AA}$ ,  $c = 18.413(1)\text{ \AA}$ ,  $\beta = 100.34(1)^\circ$ ,  $Z = 4$ ; **1b** is monoclinic,  $C2/c$ ,  $a = 11.047(1)\text{ \AA}$ ,  $b = 13.423(1)\text{ \AA}$ ,  $c = 21.933(1)\text{ \AA}$ ,  $\beta = 103.49(1)^\circ$ ,  $Z = 4$ ; **2b** is monoclinic,  $C2/c$ ,  $a = 28.589(1)\text{ \AA}$ ,  $b = 7.223(1)\text{ \AA}$ ,  $c = 14.983(1)\text{ \AA}$ ,  $\beta = 118.90(1)^\circ$ ,  $Z = 4$ .

## Introduction

Interest in lanthanide–transition-metal carbonyl complexes over the last 30 years has been prompted by the elucidation of the interaction between the two metals. Of the three structural possibilities, the most extensive class includes compounds possessing an isocarbonyl linkage between the metals.<sup>1</sup> Compounds with a direct lanthanide–transition-metal bond are uncommon,<sup>2</sup> and the unique metal–metal bond has been confirmed in only a few instances by single-crystal X-ray diffraction.<sup>3,4</sup> Another heterometallic category is characterized by a solvent-separated ion pair relationship, which has a lanthanide cation isolated from

the transition-metal carbonylate anion by a coordinating solvent.<sup>1m,5</sup>



Complexes in these three categories offer the possibility of functioning as catalyst precursors.<sup>1e,k,6,7</sup> For instance, this laboratory has been employing  $\{(\text{DMF})_{10}\text{Yb}_2[\text{Pd}(\text{CN})_4]_3\}_\infty$  as a heterogeneous bimetallic catalyst precursor in the reduction of  $\text{NO}_x$  by  $\text{CH}_4$  in the presence of  $\text{O}_2$  and in the selective vapor-phase hydrogenation of phenol into cyclohexanone.<sup>8</sup>

In light of their potential in catalysis and their diverse structural motifs, we are interested in synthesizing new

\* Author to whom correspondence should be addressed. E-mail: shore.1@osu.edu.

heterometallic carbonyl compounds by means of the metal exchange reaction or transmetalation. Previously, exchange reactions of metallic Zn or Cd with  $\text{Hg}[\text{Co}(\text{CO})_4]_2$  were shown to produce the corresponding  $\text{M}[\text{Co}(\text{CO})_4]_2$  ( $\text{M} = \text{Zn}, \text{Cd}$ ) derivatives, containing linear covalent  $\text{Co}-\text{M}-\text{Co}$  bonds.<sup>9</sup> In an analogous manner, electropositive lanthanide metals reduce and subsequently replace  $\text{Hg}(\text{II})$  in  $\text{Hg}[\text{Co}(\text{CO})_4]_2$  in THF to generate systems formulated as  $(\text{THF})_x\text{Ln}[\text{Co}(\text{CO})_4]_2$  ( $\text{Ln} = \text{Sm}, \text{Eu}, x = 4; \text{Ln} = \text{Yb}, x = 3$ )<sup>1h,i</sup> and  $(\text{THF})_4\text{Er}[\text{Co}(\text{CO})_4]_3$ .<sup>2a</sup> This method has several advantages, namely, the air and water stability of the mercury transition-metal carbonyl reagent, mild reaction conditions, quantitative yields, and only one additional and easily removed product, elemental Hg.<sup>9</sup> Furthermore, the reaction's versatility is demonstrated by the fact that new and different complexes are formed simply by varying the lanthanide, mercury transition-metal carbonyl reagent, and/or solvent. The lack of single-crystal X-ray structural studies in this area is an additional motivation for us to revisit the transmetalation

reaction using the exceptionally good coordinating solvent pyridine.<sup>10</sup> Our results from the Yb and  $\text{Hg}[\text{Co}(\text{CO})_4]_2$  exchange reactions show that the products are solvent-separated ion pairs. However, the ion pairs are readily converted to isocarbonyl polymeric networks in toluene. These two types of interactions are structurally characterized here.

## Experimental Section

**General Comments.** All manipulations were carried out on a standard high-vacuum line or in a drybox under an atmosphere of nitrogen unless otherwise noted. Pyridine, tetrahydrofuran, and toluene were dried over sodium/benzophenone and freshly distilled prior to use. Hexane was stirred over concentrated sulfuric acid for 2 days, decanted, and washed with water. The hexane was stirred over sodium/benzophenone for 1 week and distilled into a storage bulb containing sodium/benzophenone. Celite was dried by being heated at 150 °C under dynamic vacuum for 5 h. Dicobalt octacarbonyl (Strem) was vacuum sublimed and stored cold under nitrogen. Elemental sodium was washed free of mineral oil with hexane and stored under nitrogen. Sodium hydroxide was dried by being heated at 70 °C under vacuum for 5 h. Quadrupty distilled mercury (Bethlehem Apparatus Co., Inc.), mercury(II) dichloride (Alpha Products), and ytterbium powder (Strem) were used as received. Sodium tetracarbonylcobaltate was prepared by the literature procedures.<sup>11</sup> The synthesis of  $\text{Hg}[\text{Co}(\text{CO})_4]_2$ , originally prepared by Hieber et al.<sup>12</sup> and later described by King,<sup>13</sup> was slightly modified and is detailed below. Solutions of  $\text{Hg}[\text{Co}(\text{CO})_4]_2$  that are exposed to air tend to be light sensitive. Consequently, manipulations such as filtrations were performed quickly in the dark. Elemental analyses were obtained by Galbraith Laboratories (Knoxville, TN). Samples for elemental analysis were prepared by washing the crystals with hexane and vacuum-drying them for 12 h. Elemental analyses were performed on all four compounds. However, analyses for the ion pairs **1a** and **2a** were not reproducible, and consequently, the values are not reported. The elemental percentages, when compared to the calculated values, were too low for carbon and too high for hydrogen. This is also true for the isocarbonyl **2b** (vide infra). A reason for this discrepancy may be that prolonged sample pumping caused loss of not only solvent ligands but also carbon monoxide. This would lead to degradation of the compound. Infrared spectra were recorded on a Mattson Polarix Fourier transform spectrometer with 2  $\text{cm}^{-1}$  resolution. Infrared data, in the solution and solid states, are reported in Table 1.

**X-ray Structure Determination.** Single-crystal X-ray diffraction data for **1a**, **1b**, **2a**, and **2b** were collected on a Nonius KappaCCD diffraction system, which employs graphite-monochromated  $\text{Mo K}\alpha$  radiation ( $\lambda = 0.71073 \text{ \AA}$ ). A single crystal was mounted on the tip of a glass fiber coated with Fomblin oil (a pentafluoropolyether). Crystallographic data were collected at  $-100 \text{ }^\circ\text{C}$  for **1a**,  $-80 \text{ }^\circ\text{C}$  for **2a**, and  $-123 \text{ }^\circ\text{C}$  for **1b** and **2b**. Unit cell parameters were obtained by indexing the peaks in the first 10 frames and were refined by employing the whole data set. All frames were integrated and corrected for Lorentz and polarization effects using the

- (1) (a) Crease, A. E.; Legzdins, P. *J. Chem. Soc., Chem. Commun.* **1972**, 268. (b) Crease, A. E.; Legzdins, P. *J. Chem. Soc., Dalton Trans.* **1973**, 1501. (c) Onaka, S.; Furuichi, N. *J. Organomet. Chem.* **1979**, 173, 77. (d) Tilley, T. D.; Andersen, R. A. *J. Chem. Soc., Chem. Commun.* **1981**, 985. (e) Tilley, T. D.; Andersen, R. A. *J. Am. Chem. Soc.* **1982**, 104, 1772. (f) Boncella, J. M.; Andersen, R. A. *Inorg. Chem.* **1984**, 23, 432. (g) Boncella, J. M.; Andersen, R. A. *J. Chem. Soc., Chem. Commun.* **1984**, 809. (h) Suleimanov, G. Z.; Khandozhko, V. N.; Shifrina, R. R.; Abdullaeva, L. T.; Kolobova, N. E.; Beletskaya, I. P. *Dokl. Akad. Nauk SSSR* **1984**, 277, 1407. (i) Suleimanov, G. Z.; Khandozhko, V. N.; Abdullaeva, L. T.; Shifrina, R. R.; Khalilov, K. S.; Kolobova, N. E.; Beletskaya, I. P. *J. Chem. Soc., Chem. Commun.* **1984**, 191. (j) Suleimanov, G. Z.; Khandozhko, V. N.; Petrovskii, P. V.; Mekhdiev, R. Y.; Kolobova, N. E.; Beletskaya, I. P. *J. Chem. Soc., Chem. Commun.* **1985**, 596. (k) Beletskaya, I. P.; Voskoboinikov, A. Z.; Magomedov, G. K.-I. *Metalloorg. Khim.* **1990**, 3, 516 and references therein. (l) Lin, G.; Wong, W.-T. *J. Organomet. Chem.* **1996**, 522, 271. (m) Hillier, A. C.; Liu, S. Y.; Sella, A.; Zekria, O.; Elsegood, M. R. J. *J. Organomet. Chem.* **1997**, 528, 209. (n) Hillier, A. C.; Sella, A.; Elsegood, M. R. J. *J. Chem. Soc., Dalton Trans.* **1998**, 3871.
- (2) (a) Marianelli, R. S.; Durney, M. T. *J. Organomet. Chem.* **1971**, 32, C41. (b) Marks, T. J.; Kristoff, J. S.; Alich, A.; Shriver, D. F. *J. Organomet. Chem.* **1971**, 33, C35. (c) Crease, A. E.; Legzdins, P. *J. Chem. Soc., Chem. Commun.* **1973**, 775. (d) Suleimanov, G. Z.; Beletskaya, I. P. *Dokl. Akad. Nauk SSSR* **1981**, 261, 381. (e) Beletskaya, I. P.; Suleimanov, G. Z.; Shifrina, R. R.; Mekhdiev, R. Y.; Agdamskii, T. A.; Khandozhko, V. N.; Kolobova, N. E. *J. Organomet. Chem.* **1986**, 299, 239. (f) Voskoboinikov, A. Z.; Beletskaya, I. P. *Russ. Chem. Bull.* **1997**, 46, 1789.
- (3) (a) Deng, H.; Shore, S. G. *J. Am. Chem. Soc.* **1991**, 113, 8538. (b) Deng, H.; Chun, S.-H.; Florian, P.; Grandinetti, P. J.; Shore, S. G. *Inorg. Chem.* **1996**, 35, 3891.
- (4) (a) Magomedov, G. K.-I.; Voskoboinikov, A. Z.; Chuklanova, E. B.; Gusev, A. I.; Beletskaya, I. P. *Metalloorg. Khim.* **1990**, 3, 706. (b) Beletskaya, I. P.; Voskoboinikov, A. Z.; Chuklanova, E. B.; Kirillova, N. I.; Shestakova, A. K.; Parshina, I. N.; Gusev, A. I.; Magomedov, G. K.-I. *J. Am. Chem. Soc.* **1993**, 115, 3156.
- (5) (a) Evans, W. J.; Bloom, I.; Grate, J. W.; Hughes, L. A.; Hunter, W. E.; Atwood, J. L. *Inorg. Chem.* **1985**, 24, 4620. (b) White, J. P., III; Deng, H.; Boyd, E. P.; Gallucci, J.; Shore, S. G. *Inorg. Chem.* **1994**, 33, 1685. (c) Deng, D.; Zheng, X.; Qian, C.; Sun, J.; Dormond, A.; Baudry, D.; Visseaux, M. *J. Chem. Soc., Dalton Trans.* **1994**, 1665.
- (6) Beletskaya, I. P.; Voskoboinikov, A. Z.; Magomedov, G. K.-I. *Metalloorg. Khim.* **1989**, 2, 814.
- (7) (a) Imamura, H.; Igawa, K.; Kasuga, Y.; Sakata, Y.; Tsuchiya, S. *J. Chem. Soc., Faraday Trans.* **1994**, 90, 2119. (b) Imamura, H.; Igawa, K.; Sakata, Y.; Tsuchiya, S. *Bull. Chem. Soc. Jpn.* **1996**, 69, 325. (c) Imamura, H.; Miura, Y.; Fujita, K.; Sakata, Y.; Tsuchiya, S. *J. Mol. Catal. A* **1999**, 140, 81.
- (8) (a) Rath, A.; Aceves, E.; Mitome, J.; Liu, J.; Ozkan, U. S.; Shore, S. G. *J. Mol. Catal. A* **2001**, 165, 103. (b) Shore, S. G.; Ding, E.; Park, C.; Keane, M. A. *Catal. Commun.* **2002**, 3, 77.
- (9) Burlitch, J. M.; Ferrari, A. *Inorg. Chem.* **1970**, 9, 563.
- (10) White, J. P., III; Deng, H.; Shore, S. G. *Inorg. Chem.* **1991**, 30, 2337.
- (11) (a) Ruff, J. K.; Schlientz, W. *J. Inorg. Synth.* **1974**, 15, 84. (b) Edgell, W. F.; Lyford, J., IV. *Inorg. Chem.* **1970**, 9, 1932.
- (12) Heiber, W.; Fischer, E. O.; Böckley, E. *Z. Anorg. Allg. Chem.* **1952**, 269, 308.
- (13) King, R. B. In *Organometallic Syntheses*; Eisch, J. J., King, R. B., Eds.; Academic Press: New York, 1965; Vol. 1, pp 101–2.

**Table 1.** Infrared Data in the Carbonyl Stretching Frequency Region

compound	medium	$\nu(\text{CO}), \text{cm}^{-1}$
Hg[Co(CO) <sub>4</sub> ] <sub>2</sub>	Pyr	2071 (mw, sh), 2050 (ms), 2037 (mw, sh), 1978 (vs, br)
	THF	2087 (w, sh), 2063 (s), 2041 (w, sh), 1996 (vs)
Na[Co(CO) <sub>4</sub> ] <b>1a</b>	THF <sup>d</sup>	2003 (vw), 1899 (s), 1886 (s), 1855 (m, sh)
	Pyr	1888 (s)
<b>2a</b>	KBr	2054 (vw, sh), 2006 (mw, sh), 1978 (m, sh), 1881 (vs, br), 1795 (m, sh)
	THF <sup>b</sup>	1898 (s), 1887 (s, sh), 1854 (m, sh)
	THF <sup>c</sup>	2052 (vw), 2015 (m), 2006 (mw, sh), 1974 (mw), 1920 (vs), 1899 (s, sh), 1888 (s, sh), 1847 (m, sh), 1789 (s, br)
Yb[Co(CO) <sub>4</sub> ] <sub>2</sub> ·3THF <b>1b</b>	THF <sup>d</sup>	2045 (w), 2020 (s), 2010 (m), 1915 (s), 1898 (s), 1805 (s), 1785 (s)
	Tol	2050 (vw), 2019 (m), 1935 (ms, sh), 1902 (s), 1776 (mw, br)
<b>2b</b>	Pyr	1888 (s)
	KBr	2056 (mw, sh), 2017 (m, sh), 1972 (ms, sh), 1886 (vs, br), 1797 (m, sh)
	Tol	2115 (w), 2068 (mw), 2050 (m), 2023 (vs), 2003 (m, sh), 1926 (m), 1892 (m), 1847 (vw, sh), 1784 (m, br)
	THF <sup>e</sup>	2064 (vw, sh), 2052 (vw), 2012 (vw, sh), 1994 (w), 1967 (vw), 1896 (s), 1887 (s, sh), 1858 (m)
	THF <sup>f</sup>	2015 (m), 2005 (vw, sh), 1971 (w), 1921 (vs), 1900 (s, sh), 1887 (s, sh), 1848 (mw, sh), 1789 (s, br)
KBr	2021 (vs), 1965 (ms, sh), 1923 (ms, sh), 1847 (s), 1799 (ms, sh)	

<sup>a</sup> Reference 19b. <sup>b</sup> 0.0013 M solution. <sup>c</sup> 0.021 M solution. <sup>d</sup> References 1h,i and 2e. <sup>e</sup> Relatively dilute solution. <sup>f</sup> Relatively concentrated solution.

DENZO-SMN package (Nonius BV, 1999).<sup>14</sup> Absorption correction was applied using the SORTAV program<sup>15</sup> provided by MaXus software.<sup>16</sup> The positions of the heavy atoms ytterbium and cobalt were revealed by the Patterson method. The structures were refined using the SHELXTL-97 (difference electron density calculation, full-matrix least-squares refinements) structure solution package.<sup>17</sup> Data merging was performed using the data preparation program supplied by SHELXTL-97. After all non-hydrogen atoms were located and refined anisotropically, hydrogen atoms on the solvent ligands were calculated assuming standard geometries. A molecule of pyridine cocrystallized with **1a**, and a molecule of toluene cocrystallized with [(THF)<sub>2</sub>Yb{( $\mu$ -CO)<sub>3</sub>Co(CO)}<sub>2</sub>]. The toluene of crystallization in **2b** is disordered. The center of the molecule resides on a 2-fold axis. The methyl group occupies two separate off-axis sites. Each site is related by the 2-fold axis, and the occupancy of each is 50%.

**Preparation of Hg[Co(CO)<sub>4</sub>]<sub>2</sub>.** A solution of HgCl<sub>2</sub> (prepared by dissolving 1.165 g, 4.291 mmol, in 5 mL of THF) was added dropwise to a 50 mL THF solution of Na[Co(CO)<sub>4</sub>] (prepared from 1.416 g, 4.141 mmol, of Co<sub>2</sub>(CO)<sub>8</sub>). The reaction mixture was stirred for 3 h, and the solution turned a cloudy green-orange. Solvent was removed under reduced pressure. The resulting solid was exposed to air, dissolved in 20 mL of acetone, and filtered to remove NaCl. About 75 mL of distilled water was added to the filtrate to cause precipitation of Hg[Co(CO)<sub>4</sub>]<sub>2</sub>. The product was collected by vacuum filtration and washed with 15 mL of water. The golden orange solid (1.410 g, 63% yield) was recrystallized from 60 mL of hexane and was dried overnight on the vacuum line. Hg[Co(CO)<sub>4</sub>]<sub>2</sub> was stored at -40 °C in the drybox refrigerator.

**Preparation of [Yb(Pyr)<sub>6</sub>][Co(CO)<sub>4</sub>]<sub>2</sub>, **1a**.** A 50 mL flask was charged with 149 mg (0.275 mmol) of Hg[Co(CO)<sub>4</sub>]<sub>2</sub> and 50 mg (0.29 mmol) of Yb powder. Approximately 15 mL of pyridine was condensed into the flask at -78 °C. The system was warmed to room temperature and stirred overnight. During this time, the solution became dark wine red and Hg appeared. The solution was

filtered through Celite, and the solvent was removed, producing a dark, sticky red oil. Even after pumping overnight, an oil remained and the yield was not measured. A few dark brown chunklike crystals of **1a** were grown from a concentrated pyridine solution (slow evaporation at room temperature until 1 mL of solution remained). More than 2 months was required for X-ray-quality crystals to grow.

**Preparation of [Yb(THF)<sub>6</sub>][Co(CO)<sub>4</sub>]<sub>2</sub>, **2a**.** In a procedure similar to the preparation of **1a**, 130 mg (0.240 mmol) of Hg[Co(CO)<sub>4</sub>]<sub>2</sub> and 43 mg (0.25 mmol) of Yb were reacted in 20 mL of THF. After filtration, the solution was pale yellow. Removal of the solvent left a light brown solid. Clear and colorless crystals of **2a** were grown from a concentrated THF solution (slow evaporation at room temperature until 2 mL of solution remained). Crystals appeared within 24 h in a dark orange-red solution. The mother liquor was removed, and the crystals were washed with 5 mL of hexane. The crystals were dried on the vacuum line, yielding 112 mg (49% yield) of **2a**.

**Preparation of [(Pyr)<sub>4</sub>Yb{( $\mu$ -CO)<sub>2</sub>Co(CO)<sub>2</sub>}<sub>2</sub>]<sub>∞</sub>, **1b**.** Approximately 20 mL of toluene was added to the dark red oil containing **1a** (from 149 mg, 0.275 mmol of Hg[Co(CO)<sub>4</sub>]<sub>2</sub>). After the mixture was stirred for 2 h, the volatile materials were removed under vacuum. This procedure was repeated. Finally, the solid was extracted with 20 mL of toluene. Large orange blocklike crystals in a dark red solution were grown in 1 week from a concentrated toluene solution (slow evaporation at room temperature until 5 mL of solution remained). The mother liquor was removed, and the crystals were washed with 1 mL of toluene and 5 mL of hexane. The crystals were dried on the vacuum line, giving 105 mg (46% yield) of **1b**. Anal. Calcd for C<sub>24.25</sub>H<sub>16.25</sub>N<sub>3.25</sub>O<sub>8</sub>YbCo<sub>2</sub> (loss of 0.75 pyridine ligand): C, 37.72; H, 2.12; N, 5.89. Found: C, 37.44; H, 2.37; N, 6.48. Dissolving **1b** in pyridine produced a dark red wine solution.

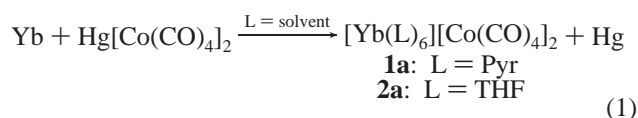
**Preparation of [(THF)<sub>2</sub>Yb{( $\mu$ -CO)<sub>3</sub>Co(CO)}<sub>2</sub>·Tol]<sub>∞</sub>, **2b**.** Approximately 20 mL of toluene was added to the light brown solid **2a** (from 156 mg, 0.288 mmol of Hg[Co(CO)<sub>4</sub>]<sub>2</sub>). After the mixture was stirred for 2 h, the volatile materials were removed under vacuum. This procedure was repeated. The light red-brown solid was extracted with 30 mL of toluene. Colorless rectangular platelike crystals in a brown oil were grown from a concentrated toluene solution (slow evaporation at room temperature until 5 mL of solution remained). The mother liquor was removed, and the crystals were washed with 1 mL of toluene and 5 mL of hexane. The crystals were dried on the vacuum line to afford 53 mg (25% yield) of **2b**. Anal. Calcd for C<sub>18</sub>H<sub>14</sub>O<sub>8.75</sub>YbCo<sub>2</sub> (loss of 1.25 THF ligands based

- (14) Otwinoski, Z.; Minor, W. In *Methods in Enzymology*; Carter, C. W., Jr., Sweet, R. M., Eds.; Academic Press: New York, 1997; Vol. 276 (A), p 307.
- (15) (a) Blessing, R. H. *Acta Crystallogr., Sect. A* **1995**, *51*, 33. (b) Blessing, R. H. *J. Appl. Crystallogr.* **1997**, *30*, 421.
- (16) Mackay, S.; Gilmore, C. J.; Edwards, C.; Tremayne, M.; Stuart, N.; Shankland, K. *MaXus: A Computer Program for the Solution and Refinement of Crystal Structures from Diffraction Data*; University of Glasgow: Glasgow, Scotland; Nonius BV: Delft, The Netherlands; MacScience Co. Ltd.: Yokohama, Japan, 1998.
- (17) Sheldrick, G. M. *SHELXTL-97: A Structure Solution and Refinement Program*; University of Göttingen: Göttingen, Germany, 1998.

on Yb and Co): C, 32.70; H, 2.13; Yb, 26.17; Co, 17.83. Found: C, 24.16; H, 3.23; Yb, 26.19; Co, 18.53.<sup>18</sup> The Yb:Co ratio is 1.00:2.08. Dissolving **2b** in THF produced a brown solution.

## Results and Discussion

**Solvent-Separated Ion Pairs. Syntheses and IR Spectra of [Yb(L)<sub>6</sub>][Co(CO)<sub>4</sub>]<sub>2</sub> (1a, L = Pyr; 2a, L = THF).** Transmetalation reactions of ytterbium metal with Hg[Co(CO)<sub>4</sub>]<sub>2</sub> in the coordinating solvents pyridine and THF afford the salts [Yb(Pyr)<sub>6</sub>][Co(CO)<sub>4</sub>]<sub>2</sub> (**1a**) and [Yb(THF)<sub>6</sub>][Co(CO)<sub>4</sub>]<sub>2</sub> (**2a**) (eq 1).



In these reactions, metallic Yb is oxidized to Yb(II) with concurrent reduction of Hg(II) to elemental Hg. Although Yb metal has low solubility in the above coordinating solvents, the precipitation of Hg drives the reaction to completion within 12 h. The resulting divalent Yb cations are encapsulated in a solvent shell and, consequently, are not directly bonded to the [Co(CO)<sub>4</sub>]<sup>−</sup> anions.

Detailed studies by Edgell and co-workers have demonstrated that a solvent's electron-donating ability influences the degree of separation between the cation (i.e., Na<sup>+</sup>) and the [Co(CO)<sub>4</sub>]<sup>−</sup> anion in solution.<sup>19</sup> Similar ion-pairing effects were observed for Yb[Co(CO)<sub>4</sub>]<sub>2</sub>. Pyridine, a stronger Lewis base than tetracarbonylcobaltate, bonds solely to the Yb<sup>2+</sup> ion, causing the appearance of one strong CO stretch at 1888 cm<sup>−1</sup> in the solution IR spectrum of **1a**. This stretch is consistent with the unperturbed tetrahedral symmetry of the isolated or solvent-surrounded [Co(CO)<sub>4</sub>]<sup>−</sup> anion.<sup>19</sup> The corresponding [Co(CO)<sub>4</sub>]<sup>−</sup> anions of the [Ln(DIME)<sub>3</sub>]<sup>2+</sup> cations (Ln = Sm, Yb; DIME = (CH<sub>3</sub>OCH<sub>2</sub>CH<sub>2</sub>)<sub>2</sub>O, diethylene glycol dimethyl ether) exhibit a similar single CO absorption in solution.<sup>5b</sup>

On the other hand, the comparable Lewis basicities of THF and [Co(CO)<sub>4</sub>]<sup>−</sup> generate peculiar features in the solution IR spectra of **2a** (Figure 1, Table 1).<sup>20</sup> Spectra of dilute THF solutions (0.0013 M) resemble those of Na[Co(CO)<sub>4</sub>] in THF. Similar to pyridine, the absorption at 1887 cm<sup>−1</sup> corresponds to the CO stretch of the solvent-separated ion pair. However, contact ion pair formation through a weak isocarbonyl interaction (i.e., [(THF)<sub>x</sub>Yb⋯OCCo(CO)<sub>3</sub>]<sup>+</sup>) reduces the symmetry of the [Co(CO)<sub>4</sub>]<sup>−</sup> anion and causes the appearance of two shoulders (1854 and 1898 cm<sup>−1</sup>) on the 1887 cm<sup>−1</sup> stretch.<sup>19</sup> This equilibrium between the solvent-separated and weak contact ion pairs in THF solutions of **2a** or Na[Co(CO)<sub>4</sub>] is ascribed to the similar electron-donating abilities of THF and [Co(CO)<sub>4</sub>]<sup>−</sup>.<sup>20</sup>

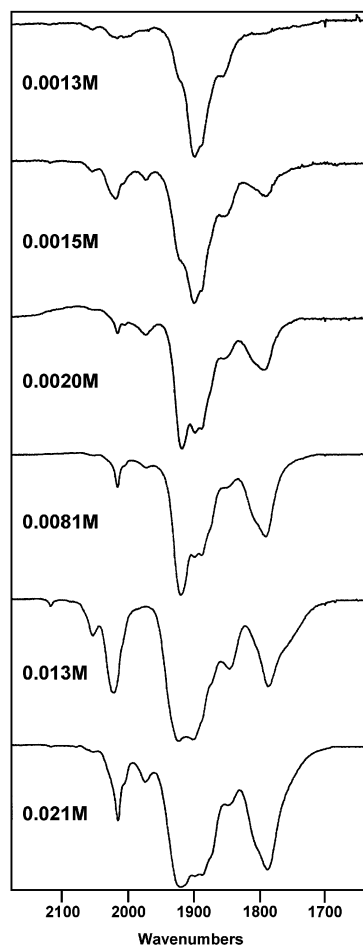


**Figure 1.** THF solution IR spectra of [Yb(THF)<sub>6</sub>][Co(CO)<sub>4</sub>]<sub>2</sub> (**2a**) as a function of concentration.

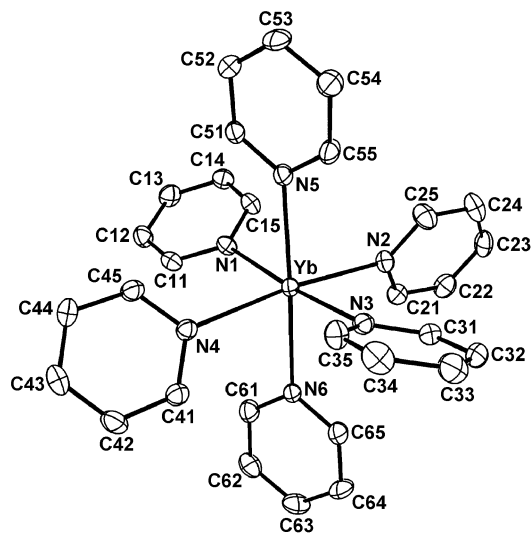
Besides the bands associated with the solvent-separated and weak contact ion pairs, additional absorptions arise in concentrated THF solution spectra of **2a** (Figure 1). The emergence of at least three new peaks is easily perceptible: two terminal CO absorptions at 2015 and 1920 cm<sup>−1</sup> and a broad distinctive bridging CO stretch at 1789 cm<sup>−1</sup> (0.021 M). The solution structure or identity of the species that produce these particular absorptions is not conspicuous, though clearly they are in equilibrium with the solvent-separated and weak contact ion pairs. A pronounced interaction (greater than the weak contact ion pair) between the Yb<sup>2+</sup> cation and carbonyl oxygens distorts the *T<sub>d</sub>* symmetry of [Co(CO)<sub>4</sub>]<sup>−</sup>, gives rise to the low-frequency CO band, and shifts the terminal CO stretches to higher frequencies. This type of concentration dependence is not manifested in the Na[Co(CO)<sub>4</sub>]/THF system since the number of ion pairs remains constant over the concentration range.<sup>19a,c</sup> Furthermore, the stronger Lewis acidity of Yb<sup>2+</sup> compared to Na<sup>+</sup> fosters greater competition between THF and [Co(CO)<sub>4</sub>]<sup>−</sup> for binding to the metal ion.

Earlier Beletskaya and co-workers produced Yb[Co(CO)<sub>4</sub>]<sub>2</sub>·3THF via transmetalation (i.e., eq 1) with precipitation of the complex by hexane.<sup>1h,i,2e</sup> The solution IR spectrum of this compound in THF has several CO stretches, but

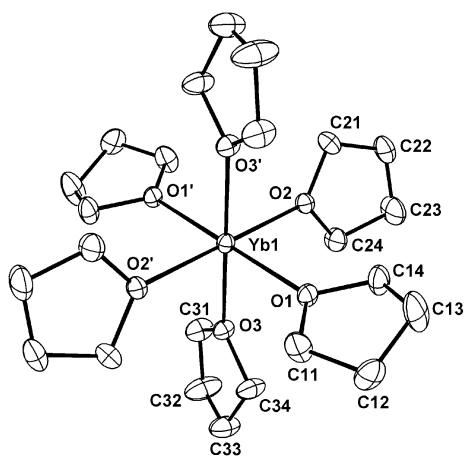
(18) Repeated analyses resulted in lower than expected carbon percentages. Due to the presence of the toluene of crystallization, it was difficult to accurately calculate the number of THF ligands lost.

(19) (a) Edgell, W. F.; Yang, M. T.; Koizumi, N. *J. Am. Chem. Soc.* **1965**, *87*, 2563. (b) Edgell, W. F.; Lyford, J., IV. *J. Am. Chem. Soc.* **1971**, *93*, 6407. (c) Edgell, W. F. In *Ions and Ion Pairs in Organic Reactions*; Szwarc, M., Ed.; Wiley-Interscience: New York, 1972; Vol. 1, Chapter 4, pp 153–176.

(20) Darensbourg, M. Y. *Prog. Inorg. Chem.* **1985**, *33*, 221.



(a)



(b)

**Figure 2.** Molecular structures of the cations in (a)  $[\text{Yb}(\text{Pyr})_6][\text{Co}(\text{CO})_4]_2$  (**1a**) (25% thermal ellipsoids) and (b)  $[\text{Yb}(\text{THF})_6][\text{Co}(\text{CO})_4]_2$  (**2a**) (15% thermal ellipsoids). Hydrogens attached to carbon atoms are omitted for clarity.

specifically the bridging carbonyl absorption at  $1785\text{ cm}^{-1}$  coincides with that of **2a** in THF at high concentrations (Table 1).

**X-ray Structures of 1a and 2a.** Crystals of **1a** and **2a** were grown from saturated solutions in the corresponding coordinating solvent. Crystals of **1a** tend to grow very slowly, taking 2 months. A molecule of pyridine cocrystallizes with **1a**. Molecular structures of these salts are illustrated in Figure 2. Crystallographic data and selected bond distances and bond angles are given in Tables 2 and 3.

The coordination geometry about the  $\text{Yb}^{2+}$  cation in **1a** is approximately octahedral (Figure 2a). Two pyridine molecules, containing the N5 and N6 atoms, are nearly coplanar and can be considered the axial ligands. The equatorial pyridine molecules are arranged in a four-blade propeller-like fashion. The Yb–N bond lengths range from 2.489(3) to 2.517(3) Å. To the best of our knowledge, only a few  $\text{Yb}^{2+}$  octahedral complexes have been reported.<sup>10,21</sup> The

**Table 2.** Crystallographic Data for  $[\text{Yb}(\text{Pyr})_6][\text{Co}(\text{CO})_4]_2\cdot\text{Pyr}$  (**1a**·Pyr),  $[\text{Yb}(\text{THF})_6][\text{Co}(\text{CO})_4]_2$  (**2a**),  $[\text{Pyr}_4\text{Yb}\{\mu\text{-CO}\}_2\text{Co}(\text{CO})_2]_2$  (**1b**), and  $[(\text{THF})_2\text{Yb}\{\mu\text{-CO}\}_2\text{Co}(\text{CO})_2]_2\cdot\text{ToI}]_\infty$  (**2b**)

	<b>1a</b> ·Pyr	<b>2a</b>	<b>1b</b>	<b>2b</b>
empirical formula	$\text{C}_{43}\text{H}_{35}\text{Co}_2\text{N}_7\text{O}_8\text{Yb}$	$\text{C}_{32}\text{H}_{48}\text{Co}_2\text{O}_{14}\text{Yb}$	$\text{C}_{28}\text{H}_{20}\text{Co}_2\text{N}_4\text{O}_8\text{Yb}$	$\text{C}_{23}\text{H}_{24}\text{Co}_2\text{O}_{10}\text{Yb}$
fw	1068.68	947.60	831.38	751.35
space group	$P2_1/c$ (No. 14)	$C2/c$ (No. 15)	$C2/c$ (No. 15)	$C2/c$ (No. 15)
<i>a</i> , Å	11.171(1)	17.724(1)	11.047(1)	28.589(1)
<i>b</i> , Å	11.925(1)	12.468(1)	13.423(1)	7.223(1)
<i>c</i> , Å	33.978(1)	18.413(1)	21.933(1)	14.983(1)
$\beta$ , deg	95.10(1)	100.34(1)	103.49(1)	118.90(1)
<i>V</i> , Å <sup>3</sup>	4508.4(6)	4002.8(4)	3162.6(4)	2708.5(9)
<i>Z</i>	4	4	4	4
$D_{\text{calc}}$ , g·cm <sup>-3</sup>	1.574	1.572	1.746	1.833
<i>T</i> , °C	−100	−80	−123	−123
$\mu$ , mm <sup>-1</sup>	2.842	3.195	4.021	4.685
R1 [ $I > 2\sigma(I)$ ] <sup>a</sup>	0.0309	0.0290	0.0158	0.0245
wR2 (all data) <sup>b</sup>	0.0748	0.0727	0.0366	0.0636

$$^a \text{R1} = \sum |F_o| - |F_c| / \sum |F_o|. \quad ^b \text{wR2} = \{\sum w(F_o^2 - F_c^2)^2 / \sum w(F_o^2)\}^{1/2}.$$

**Table 3.** Selected Bond Distances (Å) and Bond Angles (deg) for  $[\text{Yb}(\text{Pyr})_6][\text{Co}(\text{CO})_4]_2\cdot\text{Pyr}$  (**1a**·Pyr) and  $[\text{Yb}(\text{THF})_6][\text{Co}(\text{CO})_4]_2$  (**2a**)

<b>1a</b> ·Pyr		<b>2a</b> <sup>a</sup>	
Bond Distances			
Yb–N(1)	2.509(3)	Yb(1)–O(1)	2.382(2)
Yb–N(2)	2.508(3)	Yb(1)–O(2)	2.387(2)
Yb–N(3)	2.489(3)	Yb(1)–O(3)	2.396(3)
Yb–N(4)	2.510(3)	Co(1)–C(5)	1.747(6)
Yb–N(5)	2.517(3)	Co(1)–C(6)	1.748(5)
Yb–N(6)	2.516(3)	Co(1)–C(7)	1.747(6)
Co(1)–C(1)	1.768(5)	Co(1)–C(8)	1.736(6)
Co(1)–C(2)	1.765(5)	C(5)–O(5)	1.159(6)
Co(1)–C(3)	1.770(5)	C(6)–O(6)	1.136(5)
Co(1)–C(4)	1.759(5)	C(7)–O(7)	1.164(6)
C(1)–O(1)	1.148(5)	C(8)–O(8)	1.163(6)
C(2)–O(2)	1.150(5)		
C(3)–O(3)	1.150(5)		
C(4)–O(4)	1.156(5)		
Bond Angles			
N(1)–Yb–N(2)	90.8(1)	O(1)–Yb(1)–O(2)	90.2(1)
N(1)–Yb–N(3)	175.0(1)	O(1)–Yb(1)–O(3)	180.0(1)
N(1)–Yb–N(4)	89.1(1)	O(1)–Yb(1)–O(5)	91.41(9)
C(1)–Co(1)–C(2)	111.4(2)	C(5)–Co(1)–C(6)	110.5(2)
C(1)–Co(1)–C(3)	109.3(2)	C(5)–Co(1)–C(7)	108.7(2)
Co(1)–C(1)–O(1)	177.5(4)	Co(1)–C(5)–O(5)	179.6(5)
Co(1)–C(2)–O(2)	177.8(4)	Co(1)–C(6)–O(6)	179.3(6)
Co(1)–C(3)–O(3)	179.5(4)	Co(1)–C(7)–O(7)	180.0(7)
Co(1)–C(4)–O(4)	179.1(4)	Co(1)–C(8)–O(8)	179.0(6)

<sup>a</sup> Symmetry transformations used to generate equivalent atoms for **2a**:  $-x + 1/2, -y + 1/2, -z$ .

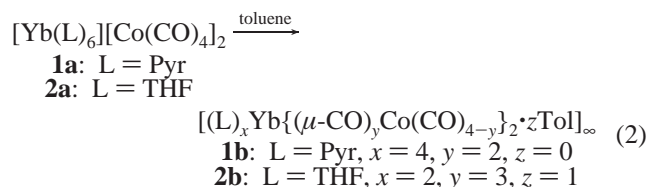
Yb–N distances in the octahedral borohydride compounds  $(\text{Pyr})_4\text{Yb}\{\mu\text{-H}\}_3\text{BH}\}_2$  (2.566(3) and 2.579(4) Å) and  $(\text{CH}_3\text{-CN})_4\text{Yb}\{\mu\text{-H}\}_3\text{BH}\}_2$  (2.520(3) and 2.529(4) Å) tend to be slightly longer than that in the homoleptic complex **1a**.<sup>10</sup> Chalcogenolates of octahedral divalent Yb,  $(\text{Pyr})_4\text{Yb}(\text{EC}_6\text{H}_5)_2$  (E = S, Se), have Yb–N distances ranging from 2.502(4) to 2.565(7) Å.<sup>21b</sup> The mixed ligand seven-coordinate cation in  $[(\text{Pyr})_5\text{Yb}(\text{CH}_3\text{CN})_2][\text{Hg}\{\text{Fe}(\text{CO})_4\}_2]_2\cdot 2\text{Pyr}$  possesses Yb–N bond lengths of 2.52(2)–2.55(2) Å (Pyr) and 2.44(2)–2.46(3) Å ( $\text{CH}_3\text{CN}$ ).<sup>5b</sup> A pentamethylcyclopentadienyl derivative of Yb(II),  $\text{Cp}^*\text{Yb}(\text{Pyr})_2$  (8-coordinate), has Yb–N distances of 2.544(6) and 2.586(7) Å.<sup>22</sup>

(21) (a) Manning, M. J.; Knobler, C. B.; Khatler, R.; Hawthorne, M. F. *Inorg. Chem.* **1991**, *30*, 2009. (b) Brewer, M.; Khanis, D.; Buretea, M.; Berardini, M.; Emge, T. J.; Brennan, J. G. *Inorg. Chem.* **1994**, *33*, 2743.

In the molecular structure of **2a**, the Yb atom resides on a special position and there are three independent THF ligands (Figure 2b). Symmetry transformations of these three ligands generate the remainder of the cation, in which the divalent Yb has a nearly octahedral coordination. The lengths of the Yb–O bonds are 2.382(2), 2.387(2), and 2.396(3) Å. A shorter distance (2.298 Å)<sup>23</sup> was reported<sup>21a</sup> for [Yb(THF)<sub>6</sub>]<sup>2+</sup> [(*nido*-7,8-C<sub>2</sub>B<sub>9</sub>H<sub>11</sub>)<sub>2</sub>]<sup>2-</sup>. Other THF-coordinated divalent organoytterbium compounds including their Yb–O bond lengths are [(MeOCH<sub>2</sub>CH<sub>2</sub>C<sub>5</sub>H<sub>4</sub>)<sub>2</sub>Yb(THF)] (2.496(4) Å; 9-coordinate),<sup>24</sup> Cp\*<sub>2</sub>Yb(THF) (2.412(5) Å; 7-coordinate),<sup>25</sup> (MeC<sub>5</sub>H<sub>4</sub>)<sub>2</sub>Yb(THF) (2.53(2) Å; 10-coordinate),<sup>26</sup> and [(Yb(Tp<sup>tBu,Me</sup>)(THF)(μ-CO)<sub>2</sub>Mo(η<sup>5</sup>-C<sub>5</sub>H<sub>4</sub>Me)(CO)<sub>3</sub>)]<sub>2</sub> (2.510(3) Å; 6-coordinate; Tp<sup>tBu,Me</sup> = hydrotris(3-(1,1-dimethylethyl)-5-methylpyrazolyl)borate).<sup>1b</sup> Also as a comparison, [Yb(DIME)<sub>3</sub>][Co(CO)<sub>4</sub>]<sub>2</sub>, which contains a tricapped trigonal prismatic arrangement of DIME ligands around the Yb<sup>2+</sup> ion, has Yb–O distances ranging between 2.49(1) and 2.69(2) Å.<sup>5b</sup>

The tetracarbonylcobaltate anions of **1a** and **2a** are not extraordinary. There are two crystallographically independent anions in **1a** and one in **2a**. Bond lengths and angles for these anions are very similar to those in other salts.<sup>5,27</sup> Only a slight distortion from the idealized tetrahedral coordination is noticeable. Average Co–C distances for **1a** and **2a** are 1.764[2] and 1.745[3] Å,<sup>28</sup> while mean C–O bond lengths measured 1.152[2] and 1.156[7] Å, respectively. The Co–C–O bond angles are nearly linear.

**Isocarbonyls. Syntheses and IR Spectra of [(L)<sub>x</sub>Yb{(μ-CO)<sub>y</sub>Co(CO)<sub>4-y</sub>}]<sub>2</sub>·zTol]<sub>∞</sub> (**1b**, L = Pyr, x = 4, y = 2, z = 0; **2b**, L = THF, x = 2, y = 3, z = 1).** Transformation of the solvent-separated ion pairs **1a** and **2a** into the isocarbonyl compounds [(Pyr)<sub>4</sub>Yb{(μ-CO)<sub>2</sub>Co(CO)<sub>2</sub>}]<sub>∞</sub> (**1b**) and [(THF)<sub>2</sub>Yb{(μ-CO)<sub>3</sub>Co(CO)<sub>1</sub>}]<sub>∞</sub> (**2b**) is facilitated by the noncoordinating solvent toluene (eq 2). Structural elucidation of **1b** and **2b** is aided by single-crystal X-ray analyses.



Stirring **1a** or **2a** in toluene (**1a** and **2a** are only slightly soluble) and removing the volatile species cause displacement

**Table 4.** Selected Bond Distances (Å) and Bond Angles (deg) for [(Pyr)<sub>4</sub>Yb{(μ-CO)<sub>2</sub>Co(CO)<sub>2</sub>}]<sub>∞</sub> (**1b**) and [(THF)<sub>2</sub>Yb{(μ-CO)<sub>3</sub>Co(CO)<sub>1</sub>}]<sub>∞</sub> (**2b**)

<b>1b<sup>a</sup></b>		<b>2b<sup>b</sup></b>	
Bond Distances			
Yb(1)–N(1)	2.589(2)	Yb(1)–O(11)	2.403(3)
Yb(1)–N(2)	2.582(2)	Yb(1)–O(1D)	2.492(3)
Yb(1)–O(1B)	2.545(2)	Yb(1)–O(2B)	2.564(3)
Yb(1)–O(4)	2.540(2)	Yb(1)–O(4)	2.522(3)
Co(1)–C(1)	1.746(2)	Co(1)–C(1)	1.745(4)
Co(1)–C(2)	1.773(3)	Co(1)–C(2)	1.756(4)
Co(1)–C(3)	1.768(3)	Co(1)–C(3)	1.789(5)
Co(1)–C(4)	1.743(2)	Co(1)–C(4)	1.751(4)
C(1)–O(1)	1.166(3)	C(1)–O(1)	1.170(5)
C(2)–O(2)	1.146(3)	C(2)–O(2)	1.156(5)
C(3)–O(3)	1.148(3)	C(3)–O(3)	1.143(6)
C(4)–O(4)	1.169(3)	C(4)–O(4)	1.162(5)
Bond Angles			
O(4)–Yb(1)–N(2)	75.32(5)	O(11)–Yb(1)–O(11A)	105.4(1)
O(1A)–Yb(1)–N(1)	143.70(6)	O(11)–Yb(1)–O(1D)	94.58(9)
N(2)–Yb(1)–N(1)	80.88(6)	O(11)–Yb(1)–O(4)	74.23(9)
O(4)–Yb(1)–N(1)	78.06(6)	O(4)–Yb(1)–O(4A)	134.6(1)
Yb(1)–O(1A)–C(1A)	153.4(2)	Yb(1)–O(1E)–C(1E)	149.9(3)
Yb(1)–O(4)–C(4)	153.2(2)	Yb(1)–O(2B)–C(2B)	141.1(3)
Co(1)–C(1)–O(1)	178.1(2)	Yb(1)–O(4)–C(4)	138.5(3)
Co(1)–C(2)–O(2)	178.6(3)	Co(1)–C(1)–O(1)	178.1(4)
Co(1)–C(3)–O(3)	179.5(2)	Co(1)–C(2)–O(2)	177.5(3)
Co(1)–C(4)–O(4)	177.7(2)	Co(1)–C(3)–O(3)	179.6(5)
C(1)–Co(1)–C(2)	109.4(1)	Co(1)–C(4)–O(4)	177.0(4)
C(1)–Co(1)–C(3)	111.7(1)	C(1)–Co(1)–C(2)	111.8(2)
C(1)–Co(1)–C(4)	110.7(1)	C(1)–Co(1)–C(3)	109.8(2)
		C(1)–Co(1)–C(4)	109.1(2)

<sup>a</sup> Symmetry transformations used to generate equivalent atoms for **1b**: (A)  $x - 1/2, y + 1/2, z$ ; (B)  $-x + 1/2, y + 1/2, -z + 1/2$ ; (C)  $-x, y, -z + 1/2$ . <sup>b</sup> Symmetry transformations used to generate equivalent atoms for **2b**: (A)  $-x + 1, y, -z + 1/2$ ; (B)  $-x + 1, -y + 1, -z + 1$ ; (C)  $x, -y + 1, z - 1/2$ ; (D)  $x, y - 1, z$ ; (E)  $-x + 1, y - 1, -z + 1/2$ .

of some solvent ligands. The Lewis basic carbonyl oxygen atoms fill the vacant coordination sites on the Lewis acidic Yb<sup>2+</sup> ions left by the partially removed solvent. The results of these isocarbonyl interactions are the two-dimensional infinite sheetlike arrays **1b** and **2b**. These two complexes belong to a rare class of lanthanide–transition-metal carbonyl extended polymeric structures, only three others of which, [(CH<sub>3</sub>CN)<sub>3</sub>YbFe(CO)<sub>4</sub>]<sub>∞</sub>,<sup>3</sup> {[(CH<sub>3</sub>CN)<sub>3</sub>YbFe(CO)<sub>4</sub>]<sub>2</sub>·CH<sub>3</sub>CN}<sub>∞</sub>,<sup>3</sup> and [Cp\*<sub>2</sub>Yb{(μ-CO)<sub>3</sub>Mn(CO)<sub>2</sub>}]<sub>∞</sub>,<sup>1f</sup> have been structurally characterized.

Toluene solution IR spectra of **1b** and **2b** indicate that both terminal and bridging carbonyls are present (Table 1). The spectrum of **1b** contains fewer CO absorptions than does that of **2b** in toluene. Four terminal CO stretches from 2050 to 1902 cm<sup>-1</sup> and one low-frequency isocarbonyl stretch at 1776 cm<sup>-1</sup> are evident for **1b**. There are several auxiliary terminal stretches ranging between 2115 and 1892 cm<sup>-1</sup> in the spectrum of **2b**. A broad isocarbonyl stretch at 1784 cm<sup>-1</sup> is also notable. The frequency of this absorption for **2b** is almost the same as **2a**'s bridging CO stretch in concentrated THF solutions. The solution- and solid-state structures of the isocarbonyls **1b** and **2b** are probably inequivalent. The local symmetries around the Co(CO)<sub>4</sub> units in crystalline **1b** and **2b** are C<sub>2v</sub> and C<sub>3v</sub>, respectively. The large number of solution terminal CO stretches suggests that the arrays are

(22) Tilley, T. D.; Andersen, R. A.; Spencer, B.; Zalkin, A. *Inorg. Chem.* **1982**, *21*, 2647.

(23) No esd's were reported.

(24) Deng, D.; Qian, C.; Song, F.; Wang, Z.; Wu, G.; Zheng, P. *J. Organomet. Chem.* **1993**, *443*, 79.

(25) Tilley, T. D.; Andersen, R. A.; Spencer, B.; Ruben, H.; Zalkin, A.; Templeton, D. H. *Inorg. Chem.* **1980**, *19*, 2999.

(26) Zinnen, H. A.; Pluth, J. J.; Evans, W. J. *J. Chem. Soc., Chem. Commun.* **1980**, 810.

(27) (a) Schussler, D. P.; Robinson, W. R.; Edgell, W. F. *Inorg. Chem.* **1974**, *13*, 153. (b) Schäfer, H.; MacDiarmid, A. G. *Inorg. Chem.* **1976**, *15*, 848. (c) Fachinetti, G.; Floriani, C.; Zanazzi, P. F.; Zanzari, A. R. *Inorg. Chem.* **1978**, *17*, 3002. (d) Baenziger, N. C.; Flynn, R. M.; Holy, N. L. *Acta Crystallogr.* **1979**, *B35*, 741. (e) Calderazzo, F.; Fachinetti, G.; Marchetti, F.; Zanazzi, P. F. *J. Chem. Soc., Chem. Commun.* **1981**, 181.

(28) Stout, G. H.; Jensen, L. H. In *X-ray Structure Determination*, 2nd ed.; Wiley: New York, 1989; pp 406–408. The standard deviation ( $\sigma$ ) for the average Co–C and C–O bond lengths is calculated according to the following equation from ref 28:  $\langle l \rangle = \sum_m (l_m - \langle l \rangle)^2 / m(m - 1)^{1/2}$ , where  $\langle l \rangle$  is the mean length,  $l_m$  is the length of the  $m$ th bond, and  $m$  is the number of bonds.

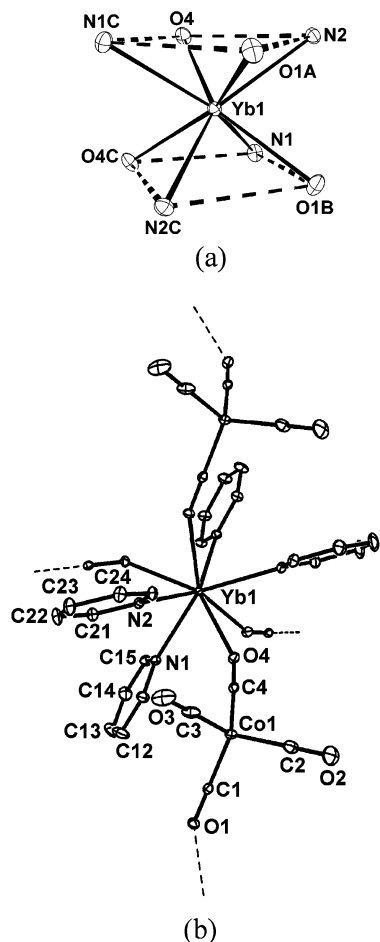


**Figure 3.** (a) Coordination geometry (25% thermal ellipsoids) about the  $\text{Yb}^{2+}$  ion in  $[(\text{Pyr})_4\text{Yb}\{\mu\text{-CO}\}_2\text{Co}(\text{CO})_2]_2$ , **1b**. (b) Molecular structure (15% thermal ellipsoids) of a portion of the two-dimensional array of **1b**. Hydrogen atoms are omitted for clarity.

dissociated into oligomeric units. In general, there is an about  $110\text{ cm}^{-1}$  difference between the terminal CO stretch for the solvent-separated ion pairs **1a** and **2a** and the bridging CO absorption for the isocarbonyls **1b** and **2b**. A similar isocarbonyl complex,  $\text{Cp}^*_2\text{Yb}(\text{THF})\{\mu\text{-CO}\}_3\text{Co}(\text{CO})_3\}$  ( $\text{Yb}^{3+}$ ), has a lowered stretch (Nujol mull) at  $1761\text{ cm}^{-1}$ .<sup>1d</sup>

Addition of pyridine to crystalline **1b** ruptures all of the isocarbonyl bridges to re-form the solvent-separated ion pair **1a**. Dissolving **2b** in THF cleaves some of the isocarbonyl linkages, but complete conversion to **2a** cannot be accomplished. Depending on the concentration, the solvent-separated ion pair **2a**, the weak contact ion pair, and the unidentified isocarbonyl compound (as well as other possible carbonyl complexes) are always in equilibrium (Table 1, Figure 1). The preceding transformations further corroborate the Lewis basicity order: pyridine  $>$  THF  $\approx$   $[\text{Co}(\text{CO})_4]^-$ .

**X-ray Structures of 1b and 2b.** Molecular structures of **1b** and **2b** are shown in Figures 3–6. Crystallographic data and selected bond distances and bond angles are given in Tables 2 and 4. A molecule of toluene cocrystallizes with  $[(\text{THF})_2\text{Yb}\{\mu\text{-CO}\}_3\text{Co}(\text{CO})_2]_2$ .

The  $\text{Yb}(\text{II})$  center in **1b** is 8-coordinate, with four pyridine ligands and four isocarbonyl linkages, forming a slightly distorted square antiprism (Figure 3a). Vertexes of the square

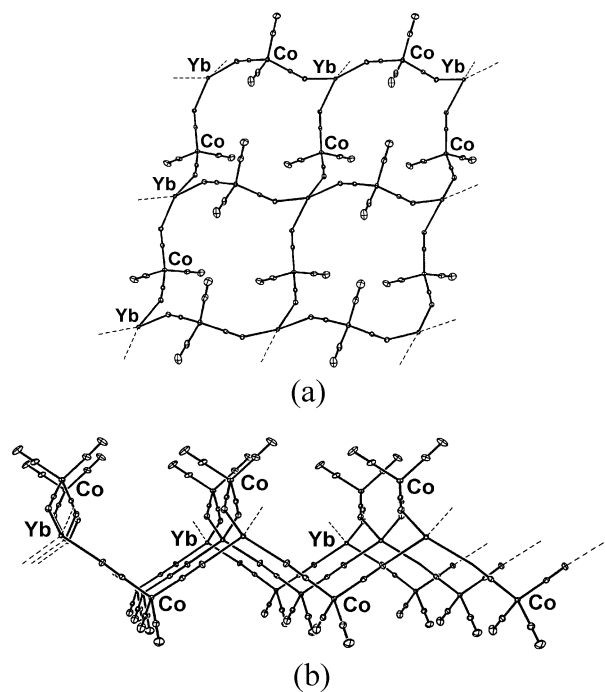


**Figure 4.** Perspectives of the two-dimensional framework (15% thermal ellipsoids) of **1b**: (a) top view and (b) cross-section. Pyridine ligands are omitted for clarity.

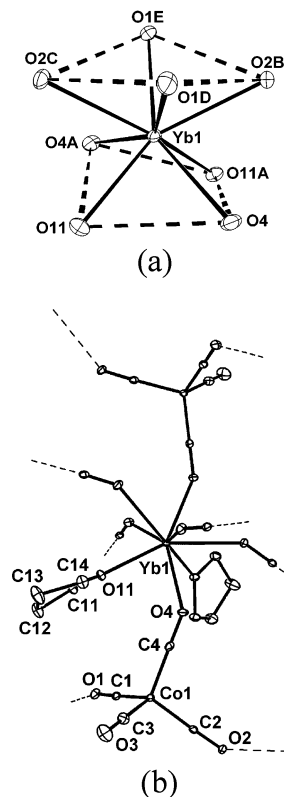


**Figure 5.** (a) Coordination geometry (25% thermal ellipsoids) about the  $\text{Yb}^{2+}$  ion in  $[(\text{THF})_2\text{Yb}\{\mu\text{-CO}\}_3\text{Co}(\text{CO})_2]_2$ , **2b**. (b) Molecular structure (15% thermal ellipsoids) of a portion of the two-dimensional array of **2b**. Hydrogen atoms are omitted for clarity.

antiprism are comprised of alternating oxygen and nitrogen atoms. The  $\text{Yb-N}$  distances are  $2.582(2)$  and  $2.589(2)\text{ \AA}$ , which are lengthened compared to those of **1a**, and the  $\text{Yb-O}$  distances are  $2.540(2)$  and  $2.545(2)\text{ \AA}$ . Two isocar-

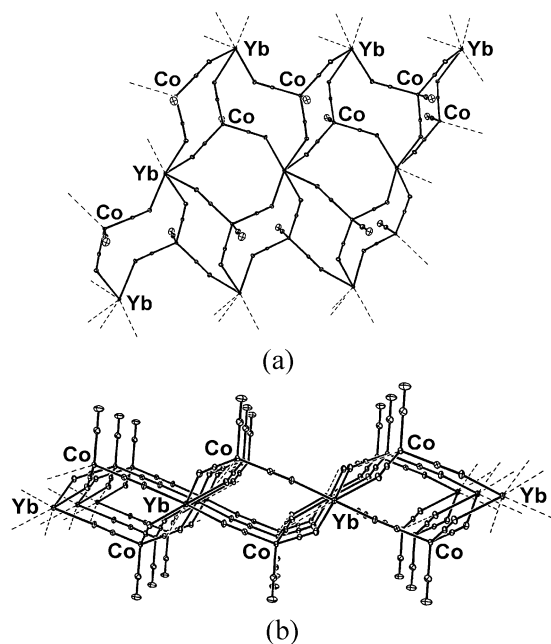


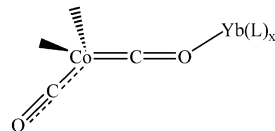
**Figure 6.** Perspectives of the two-dimensional framework (15% thermal ellipsoids) of **2b**: (a) top view and (b) cross-section. THF ligands and the toluene of crystallization are omitted for clarity.

bonyl bridges connect each cobalt to two ytterbium atoms. The two terminal carbonyls complete the nearly tetrahedral geometry of the cobalt. The ytterbium atom, two pyridine ligands, and one tetracarbonylcobaltate anion form the asymmetric unit of **1b** (Figure 3b). Symmetry transformations of these unique atoms generate the nonplanar two-dimensional polymeric sheet (Figure 4a). The isocarbonyl linkages create “eight-membered” rings, each with four ytterbium and four cobalt atoms. The corners of the rings are occupied by the ytterbium atoms. A cross-section of the zigzag pucker sheet shows that the  $\text{Co}(\text{CO})_4$  units are located above and below the plane containing the ytterbium atoms (Figure 4b).

Though the  $\text{Yb}^{2+}$  cation in **2b** has eight ligands, including six isocarbonyl oxygens and two THF molecules, its square antiprismatic geometry is more distorted than that of **1b** (Figure 5a). This distortion can be attributed to the almost 0.10–0.15 Å discrepancy between the two different types of  $\text{Yb}-\text{O}$  bond lengths. The distance of the  $\text{Yb}-\text{O}(\text{THF})$  bond is 2.403(3) Å, and the lengths of the  $\text{Yb}-\text{O}(\text{isocarbonyl})$  bonds are 2.492(3), 2.522(3), and 2.564(3) Å. The former length is a bit longer than in **2a** since the metal now has a larger coordination number. The asymmetric unit is composed of the Yb atom, one THF ligand, and one tetracarbonylcobaltate unit (Figure 5b). In contrast to **1b**, each  $\text{Co}(\text{CO})_4$  moiety participates in three isocarbonyl linkages,

thereby coupling it to three separate Yb atoms and generating “four-membered” rings with alternating ytterbium/cobalt corners (Figure 6a).

The effect, in terms of bond lengths, angles, and  $\nu_{\text{CO}}$ , of a Lewis acid interacting with a carbonyl oxygen has been reviewed.<sup>1k,20,29</sup> The bonding description for the Yb–Co isocarbonyls **1b** and **2b** may be illustrated by the following structure:



As with **1a** and **2a**,  $\pi$ -back-bonding of electron density from the filled cobalt  $d$  orbitals into the  $\pi^*$  antibonding orbitals of CO is expected for **1b** and **2b**. Donation of a lone pair of electrons on a carbonyl oxygen to an unoccupied orbital of  $\text{Yb}^{2+}$  drains electron density from CO. To compensate for this, cobalt contributes more electron density to CO. These synergistic effects induce a shortening of the bridging  $\text{Co}-\text{C}$  bonds and a lengthening of the  $\text{C}-\text{O}$  bonds relative to the terminal ones. Single-crystal X-ray diffraction data generally support these trends. Average bridging  $\text{Co}-\text{C}$  bonds in **1b** (1.745[2] Å) and **2b** (1.751[5] Å) tend to be 0.03 Å shorter than the corresponding terminal bonds (**1b**, 1.771[3] Å; **2b**, 1.789(5) Å). In contrast, mean bridging  $\text{C}-\text{O}$  distances (**1b**, 1.168[2] Å; **2b**, 1.163[7] Å) are approximately 0.02 Å longer than the terminal bonds (**1b**, 1.147[1] Å; **2b**, 1.143(6) Å). Additionally, the increased  $sp^2$ -hybridized character of the bridging oxygen is indicated by a bent  $\text{Yb}-\text{O}-\text{C}$  angle (153.3[2]° for **1b** and 143[2]° for **2b**). Other Yb–Co isocarbonyl systems,  $\text{Cp}^*_2\text{Yb}(\text{THF})\{\mu\text{-CO}\}\text{Co}(\text{CO})_3\}^{1d}$  and  $(\text{Cp}^*_2\text{Yb})_2\{\mu_3\text{-CO}\}_4\text{Co}_3(\text{C}_5\text{H}_4\text{SiMe}_3)_2\}^{1g}$  conform to these trends.

**Acknowledgment.** This work was supported by the National Science Foundation through Grant CHE99-01115. C.E.P. is grateful for generous fellowships provided by Procter & Gamble and Lubrizol.

**Supporting Information Available:** Four crystallographic files in CIF format, molecular structures of the anions in **1a** and **2a**, molecular structures of the solvents of crystallization in **1a** and **2b**, relevant solution- and solid-state IR spectra, and tables of crystallographic data. This material is available free of charge via the Internet at <http://pubs.acs.org>.

IC020254G

- (29) (a) De La Cruz, C.; Sheppard, N. *J. Mol. Struct.* **1990**, *224*, 141. (b) Horwitz, C. P.; Shriver, D. F. *Adv. Organomet. Chem.* **1984**, *23*, 219. (c) Ulmer, S. W. Ph.D. Dissertation, Cornell University, Ithaca, NY, 1972.